Therapeutic index of gramicidin S is strongly modulated by D-phenylalanine analogues at the β-turn

Concepción Solanas[†], **Beatriz G. de la Torre**[‡], **María Fernández-Reyes**[#], **Clara M. Santiveri**[§], **M. Ángeles Jiménez**[§], **Luis Rivas**[#], **Ana I. Jiménez**[†], **David Andreu**[*,‡], and **Carlos Cativiela**[*,†]

[†] *Departamento de Química Orgánica, Instituto de Ciencia de Materiales de Aragón, Universidad de Zaragoza–CSIC, 50009 Zaragoza, Spain*

[‡] *Departament de Ciències Experimentals i de la Salut, Universitat Pompeu Fabra, Dr. Aiguader 88, 08003 Barcelona, Spain*

[#] *Centro de Investigaciones Biológicas, CSIC, Ramiro de Maeztu 9, 28040 Madrid, Spain*

[§] *Instituto de Química-Física Rocasolano, CSIC, Serrano 119, 28006 Madrid, Spain*

Abstract

Analogues of the cationic antimicrobial peptide gramicidin S (GS), *cyclo*(Val-Orn-Leu-D-Phe-Pro)$_2$, with D-Phe residues replaced by different (restricted mobility, mostly) surrogates have been synthesized and used in SAR studies against several pathogenic bacteria. While all D-Phe substitutions are shown by NMR to preserve the overall β-sheet conformation, they entail subtle structural alterations that lead to significant modifications in biological activity. In particular, the analogue incorporating D-Tic (1,2,3,4-tetrahydroisoquinoline-3-carboxylic acid) shows a modest but significant increase in therapeutic index, mostly due to a sharp decrease in hemolytic effect. The fact that NMR data show a shortened distance between the D-Tic aromatic ring and the Orn δ-amino group may help explain the improved antibiotic profile of this analogue.

Keywords

Gramidicin S; cationic antimicrobial peptides; D-Phe analogues; NMR; β-sheet structure

Introduction

A remarkable increase in bacterial resistance to classical antibiotics has in recent years emerged as a major global health concern and spurred intense efforts towards the development of new antimicrobial chemotherapy approaches. A number of peptides with antimicrobial activity have been identified in a wide variety of organisms[1,2] and recognized as promising candidates against multi-drug resistant bacteria. An attractive feature of these peptides is that, by acting mostly through interaction with plasma membrane phospholipids, their developing resistance is less likely than for other mechanisms of action, since it would involve major changes in phospholipid composition that would in turn require substantial overhauling of membrane-based enzymatic and transport systems. Gramicidin S (GS) [*cyclo*(Val-Orn-Leu-D-Phe-Pro)$_2$]

(Figure 1), a cyclic decapeptide isolated from *Bacillus brevis*[3] and active against bacteria and fungi,[4,5] is one of the most widely studied antimicrobial peptides. GS adopts a full β-sheet pleated structure[6-8] where the Val, Orn and Leu residues align to form two antiparallel β-strands while D-Phe and Pro form type II′ β-turns. The structure is stabilized by four inter-strand hydrogen bonds between the Leu and Val residues and displays C_2-symmetry. The β-sheet places the hydrophobic Val and Leu side chains on a non-polar face of the GS molecule and across from the cationic Orn side chains, thus creating an amphiphilic structure that is thought to be essential for bioactivity[5,9]. Although not fully unveiled, the mechanism of action of GS sets out with a peptide-membrane interaction, leading to the disruption of the lipid bilayer and concomitant enhancement of its permeability[10], eventually resulting in cell death. Unfortunately, GS not only affects bacterial membranes, but also mammalian cells such as erythrocytes. This hemolytic activity hampers its use as a systemic antibiotic and confines it to topical administration[5].

Significant efforts have been devoted to rationalize the biological behavior of GS with the ultimate goal of generating derivatives with an improved therapeutic index. In this respect, both the β-strand[11-13] and β-turn[14-23] regions of the molecule have been the subject of modification. SAR studies on these GS analogues have identified several factors underlying the biological properties of GS: cationic charge,[10,23] amphipathic character[24,25] and β-sheet structure[23,24,26] are believed to be essential for an interaction of the peptide with lipid bilayers with some degree of specificity. In addition, global hydrophobicity provided not only by the β-sheet[27], but also by the β-turn[14-16,23,28] appears to be strongly related to the biological properties of GS. The β-turn region of GS can be successfully replaced by a variety of peptidomimetics, provided the surrogates have hydrophobic character and adequate geometry[5,15,29-31].

This paper decribes a GS analogue series generated by replacing the D-Phe residue in both β-turn regions by hitherto unexplored, Phe-related residues. Mutations at these two positions have received considerable attention[14,23,32,33] as particularly promising in the search for GS analogues with improved pharmacological profiles. We have examined the antimicrobial and hemolytic activity of these analogues along with their secondary structures by NMR and found that, aside from the β-sheet conformation, side chain packing appears to play an important role in biological activity. Thus, the analogue with the best antimicrobial-to-hemolytic activity ratio (peptide **6**, Fig. 2) in the series displays rather distinctive packing between its cationic (Orn) and aromatic (D-Tic) sites.

Results

Peptide design and synthesis

Amino acid residues selected as D-Phe replacements in GS are shown in Fig. 2. All of them have D configuration and include various modifications at the aromatic side chain such as insertion of a methylene group (Hpa, analogue **1**), or further aromatic rings in diverse arrangements (analogues **2-5**), including one (**5**) where the fluorenyl system imposes coplanarity of the two phenyl rings, with presumable conformational restriction. In a final analogue (**6**), we explored the behavior of 1,2,3,4-tetrahydroisoquinoline-3-carboxylic acid (Tic), in which a methylene unit connects the aromatic substituent to the backbone.

Solid-phase Boc chemistry protocols[18,22] were used to prepare GS and the six analogues in Fig. 2. Non-commercially available Boc-D-Flg-OH was obtained in enantiomerically pure form following our previously reported methodology.[34] In addition, the side chain of *N*-Boc ornithine was protected as a formamide as described by Kitagawa.[35] For each peptide, the synthetic route in Scheme 1 was followed. Once sequence assembly was complete, the linear decapeptide was released from the polymeric support by TFMSA acidolysis and submitted to

cyclization under high-dilution conditions. Deprotection of the Orn side chains by acid hydrolysis furnished the target peptides (GS and analogues **1–6**), which were purified by reversed-phase HPLC in satisfactory yields and high purity. All peptides were further characterized by MS and NMR.

NMR structural studies

Peptides **1-6** were investigated in aqueous solution by NMR in search for characteristic GS traits such as β-sheet conformation. Since GS and all analogues each contain two Pro residues, minor NMR signals from the *cis* conformation were observed, as expected in Pro-containing peptides. Still, the *trans-trans* rotamers were confirmed in all cases as the major species by the observation of Pro $^{13}C_\beta$ - $^{13}C_\gamma$ chemical shift differences ($\Delta\delta^{Pro} = \delta^{C\beta} - \delta^{C\gamma}$, ppm) in the 5.0–5.9 ppm range characteristic of *trans*, vs. $\Delta\delta^{Pro} \sim$ 10 ppm for *cis* Pro residues [36].

The first evidence that the analogues adopt the same structure as GS comes from the similarity of their ^{1}H, ^{13}C and ^{15}N chemical shifts with those of the parent peptide (Table ST1). The significant differences (≥ 0.2 ppm) observed for some protons are explained by anisotropy effects from the aromatic ring currents. Analogues **5** and **6** are those with larger ^{1}H chemical shift differences relative to GS, and the only ones for which some ^{13}C and ^{15}N chemical shifts also deviate considerably from GS (≥ 1.0 ppm; Table ST1).

Chemical shifts of C_αH protons and C_α carbons, given their dependence on (φ) and ψ backbone torsion angles, are good indicators of secondary structure formation. For GS (Figure 1), $\Delta\delta_{C\alpha H}$ conformational shifts ($\Delta\delta_{C\alpha H} = \delta_{C\alpha H}^{observed} - \delta_{C\alpha H}^{random\ coil}$, ppm) expected for β-strand residues Val1/1′, Orn2/2′ and Leu3/3′ are positive ($\Delta\delta_{C\alpha H} = +0.40$ ppm on average in β-sheets)[37,38] and $\Delta\delta_{C\alpha}$ conformational shifts ($\Delta\delta_{C\alpha} = \delta_{C\alpha}^{observed} - \delta_{C\alpha}^{random\ coil}$, ppm) negative (−1.6 ppm on average in β-sheets)[37]. Turn residues were excluded from this analysis as no references are available for random coil values of D-Phe*4/4′. The $\Delta\delta_{C\alpha H}$ and $\Delta\delta_{C\alpha}$ profiles of GS and peptides **1–4** and **6** are very similar and fit the expected pattern, except for Val1/1′ (Figure 3), whose anomalous C_αH chemical shifts can be explained by the strong anisotropy of the aromatic ring, as reported for some β-hairpin peptides[39]. The larger $\Delta\delta_{C\alpha H}$ and very negative $\Delta\delta_{C\alpha}$ values displayed by Leu3/3′in analogue **6** are probably due to the cyclic nature of D-Tic4/4′ leading to effects equivalent to those described for Pro-preceding residues[40]. In summary, these data confirm that peptides **1–4** and **6** in aqueous solution adopt the same backbone conformation as GS. The resemblance is not so clear-cut in the case of analogue **5**, for which $\Delta\delta_{C\alpha H}$ values for other residues than Val1/1′ also deviate from the expected behavior (Figure 3). Again, deviations are attributable to aromatic ring current effects, which in this particular peptide might differ from the rest, as the phenyl rings in D-Flg (Figure 2) are necessarily coplanar. Further confirmation about the β-sheet conformation of residues 1/1′ to 3/3′ came from their large $^3J_{C\alpha H-NH}$ coupling constants (8.2–10.0 Hz; Table ST2). Also, the small $^3J_{C\alpha H-NH}$ coupling constants of residues 4/4′ corroborate their involvement in a turn.

Indeed, the strongest evidence about the conformational features of the peptides came from NOE data. The GS β-sheet structure (Figure 1) is characterized by three NOEs involving backbone protons C_αH Orn2 – C_αH Orn2′ (distance in a canonical antiparallel β-sheet: 2.2 Å), NH Val1 – NH Leu3′, and NH Val1′ – NH Leu3 (distance in a canonical antiparallel β-sheet: 3.3 Å). Since GS and peptides **1–6** are symmetrical, the first NOE is not observable, while the last two must overlap into a single cross-peak corresponding to both NOEs. Such a cross-peak is present in the NOESY spectra of GS and peptides **1**, **3** and **6** (Table 1), demonstrating that the three analogues have GS-like β-sheet backbones. The failure to detect such a NOE in **4** and **5** precludes its use as a proof of β-sheet backbone structure, but does not necessarily exclude the presence of this conformational trait.

Aside from NOEs involving backbone protons, NOEs between Val and Leu side chain protons were observed for GS and analogues (Table 1 & Figure 4), except for **2**, probably due to low solubility. Since Val and Leu side chains pack together on the same face of the GS β-sheet, these NOEs provide additional proof of the peptides adopting GS-like β-sheet structures.

The cross-strand hydrogen bonding network in the β-sheet (NH Val1 – O Leu3′, NH Val1′– O Leu3, NH Leu3 – O Val1′, and NH Leu3′ – O Val1; see Figure 1) can be also examined by NMR. Experimental evidence for the involvement of NH amide protons in intramolecular hydrogen bonds can be obtained from NH/ND exchange rates and from temperature coefficients of the amide protons ($\Delta\delta/\delta T$). The latter are easier to measure and have long been recognized as related to solvent exposure. Accessible amide protons usually have $\Delta\delta/\delta T$ values within the −6.0 to −9.5 ppb K^{-1} range, while values above −4.5 ppb K^{-1} indicate low solvent accessibility and hence involvement in intra-molecular hydrogen bonds. As expected, solvent-exposed NH amide protons of Orn2/2′ and D-Phe*4/4′ displayed temperature coefficients below −6.5 ppb K^{-1}, with peptide **5** as single exception (Table 2). More interestingly, the low $\Delta\delta/\delta T$ absolute values for the NH amide protons of Leu3/3′ in all peptides, as well as for the NH of Val1/1′ in **6**, suggested participation in intramolecular hydrogen bonds, as expected for GS. In contrast, Val1/1′ NH amide protons in both GS and peptides **1–5** had $\Delta\delta/\delta T$ values in the range typical of solvent-accessible protons, with values larger (in absolute value) than the −9.5 ppb K^{-1} limit for peptides **3–5**. Two explanations for this behavior can be given: either (i) hydrogen bonding in Val1/1′ NH is non-existent or weaker than that of the NH of Leu3/3′, or (ii) anisotropy effects from D-Phe4/4′ (or D-Phe*4/4′) affect the Val1/1′ NH chemical shifts in both GS and **1–5**. In either case, the different behavior of Val1/1′ vs. Leu3/3′ NH protons would arise from their proximity to the turn region (Figure 1) and the ensuing disruption of the antiparallel β-sheet regularity. Such deviation from canonical β-sheet for Val1/1′ residues would also account for their anomalous $\Delta\delta_{C\alpha H}$ and $\Delta\delta_{C\alpha}$ values (see above; Figure 3).

To discern between the two alternatives the NH/ND exchange rates, which provide more definitive evidence about solvent protection and are unaffected by aromatic ring currents, were measured. Thus, the amide NH signals of Orn2/2′ and D-Phe4/4′ in GS at 5 °C disappeared shortly after dissolving the sample in D$_2$O (see Experimental Section), indicating fast solvent exchange. In contrast, NH protons of Val1/1′ and Leu3/3′ were slow-exchanging, their NMR signals remaining after >18 h. This is in agreement with the NH protons of both Val1/1′ and Leu3/3′ being hydrogen-bonded, and thus suggests that the large $\Delta\delta/\delta T$ absolute values observed for Val1/1′ NH protons are due to magnetic anisotropy. Their variability among GS and the six analogues stems from their distinctive D-Phe*4/4′ residues, each giving rise to characteristic ring current effects. In this regard, the fact that the $\Delta\delta/\delta T$ coefficient for Val1/1′ in peptide **6** has the expected value for hydrogen-bonded amide protons suggests that the side chain of D-Tic freezes the phenyl ring in an orientation that minimizes its anisotropy effects over the Val1/1′ NH proton.

Analogue **5**, for which the Val1/1′ temperature coefficient is the most negative (−23.4 ppb K^{-1}; Table 2), and that of Orn2/2′ less negative than expected for an exposed amide proton, merits further comment (Table 2 & Figure 1). The most likely explanation is that the anisotropy effects of the large, rigid aromatic D-Flg side chain strongly influence the chemical shifts of both NH protons. This is supported by the fact that the remaining analogues show very similar chemical shifts for the NH protons of Val1/1′ and Orn2/2′ (7.52–7.82 and 8.64–8.74 ppm, respectively; Table ST1), while those of **5** are quite different (8.25 and 8.31 ppm, respectively).

Having shown that analogues **1–6** adopt the same β-sheet backbone structure as the parent GS (perhaps a bit distorted for peptide **5**), we next investigated side chain packing, which is responsible for the polar/hydrophobic distribution seemingly essential for membrane interaction and hence antimicrobial and hemolytic activity. A qualitative examination of NOEs

from D-Phe*4/4′ (Table 1 & Figure 4) indicates that the aromatic rings interact with the adjacent Leu and Pro residues, both in GS and in **1–5**. For analogue **6**, in contrast, NOE data suggest that the aromatic rings interact with Orn2/2′ and retain the proximity to Leu3/3′ but not to Pro5/5′. This is confirmed by large chemical shift differences (relative to GS) of some protons of Orn2/2′ (0.4–0.6 ppm; Table ST1) and of Pro5/5′ (1.18 and 0.33 ppm for the $C_{\delta\delta'}$H protons; Table ST1), while for the side chain protons of Leu3/3′ the differences do not exceed 0.22 ppm. Proximity between the D-Tic and Orn side chains may be explained by a π-cation interaction.

To further visualize the side chain packing of peptides **1–6** relative to GS, structure calculations were performed. Due to the symmetry of GS and analogues, every observed NOE has four possible assignments. However, after our NMR analysis demonstrated that the peptides adopt the GS β-sheet structure (Figure 1), some NOE ambiguities could be solved. Thus the restraints used for structure calculation combined (i) theoretical restraints for the backbone of strand residues Val1/1′, Orn2/2′, and Leu3/3′ derived from those expected for the GS β-sheet (Figure 1; more details in the Experimental Section and the Supporting Information), and (ii) experimental distance restraints derived from the complete set of NOEs observed for each peptide. For every non-intra-residual NOE, all the existing possibilities were taken into account and the NOE assignments compatible with the GS β-sheet were identified by iterative structure calculations. The final model structures obtained for GS and peptides **1–6** (Figures 5 & SF3) are well defined, particularly for **6** (see RMSD values in Table ST3). A general examination of the structures corroborates the main conformational traits deduced from the qualitative analysis of NMR parameters. Concerning the orientation of the aromatic side chain at positions 4/4′, the phenyl rings in **1** are quite disordered and explore a much wider space than in GS, while the aromatic systems of peptides **4** and **5** adopt quite well defined positions. Also noteworthy is the different relative orientation of the two phenyl rings in D-Flg and D-Dip, in the latter case with the rings almost perpendicular to each other, and one in an orientation close to that of the D-Phe ring in GS (Figure SF3). Even more remarkable are the differences between GS and analogue **6** (Figure 5) in the relative orientation of the aromatic rings and of the positively charged Orn side chains, with noticeable consequences on their respective biological activities (see below).

Biological activity

Microbicidal activities were determined in solution, since in solid media they tend to be undermeasured, especially for Gram-negatives.[4] Two Gram-positive (*Staphylococcus aureus* and *Listeria monocytogenes*) and a Gram-negative (*Acinetobacter baummanii* ATCC 19606 and its isogenic strain resistant to polymyxin E (PXE)) bacterial strains were tested. Although GS is mostly active against Gram-positives, the occurrence of cutaneous infection by *A. baumannii* and the increasing resistance to PXE, the last universal drug active against these bacteria[41], prompted us to include both of them in the panel. Results are listed in Table 3.

Within the Gram-positive group, the tested set of analogues had better and comparable activities, respectively, for *Staphylococcus* and *Listeria* than the parental GS. In contrast, against the Gram-negative *A. baumannii*, activity in the analogue series tended to deteriorate relative to GS, more markedly so for the isogenic PXE-resistant strain. The sole exception was the D-Hpa-containing peptide **1**, which performed slightly better than GS against both PXE-sensitive and resistant strains, suggesting it is impervious to modifications in lipopolysacharide (LPS) structure.

The hemolytic effect of the peptides was evaluated on sheep erythrocytes (Table 3) as an indicator of toxicity against mammalian cells. In this assay, five (**1-5**) out of six analogues turned out to be more toxic than the parent GS. The finding that the D-Flg analogue (**5**) was more cytotoxic and yet less potent than the parent antibiotic underscores the fact that subtle

structural changes in GS may translate into different abilities to damage prokaryotic and eukaryotic cells. An opposite, though similar and more promising, segregation of antibacterial and hemolytic activities was found for **6**, which has GS-like MIC_{50} values for Gram-positives (Table 3) but is essentially harmless towards erythrocytes.

Beyond adequate intrinsic microbicidal activity, a convenient assessment of the clinical potential of an antibiotic is provided by its therapeutic index (TI, defined as HC_{50}/MIC_{50}, see Table 3), where the cytotoxic and microbicidal effects are combined. As found in previous SAR studies on GS [23,25,42,43], improved TIs are more often due to a decrease in cytotoxicity than to an increase in antibiotic potency. In the present series, the above-mentioned (higher than for GS) toxicity values, coupled with the minute, if any, improvements in microbicidal activity, resulted in TI values slightly lower or clearly worse than that of the parent structure. The sole exception to this pattern was the D-Tic analogue (**6**), for which a modest but significant improvement in TI was obtained (Table 3).

Discussion

The type II′ β-turn is a structural motif especially suited to induce alignment of its two side sequence segments into an antiparallel β-sheet. The quintessential example of this situation is GS, whose type II′ β-turns have been a testing ground for extensive D-Phe-Pro replacements by a variety of peptidomimetics, with variable success (see Introduction and refs.[29-31,44-46]). In comparison, fewer studies have addressed the substitution of either L-Pro[17,47] or D-Phe[33,46,48-50] by appropriate surrogates. The goal of this work was to explore and structurally interpret the fine-tuning of GS antibiotic activity by replacement of D-Phe with a novel set of non-coded aromatic D-amino acids already tested as turn-promoters.

The activity of GS is assumed to be somehow related to the permeabilization of bacterial membranes, though no unified opinion on the nature of such process exists[51]. Hydrophobicity has been cited as a relevant parameter[25,42,43], and inspection of the current set of D-Phe analogues (Figure 2) shows considerable variation in the number and size of aromatic side-chains, hence in overall hydrophobicity at this position. The presence of a sizable hydrophobic domain is closely related to hemolytic activity in antimicrobial peptides, as it seemingly promotes a higher partition of the peptide into biological membranes, regardless of their zwitterionic or anionic character[24,25,42]. Accordingly, the hemolytic and Gram-positive microbicidal activities run somewhat parallel, provided hydrophobicity does not drastically reduce peptide solubility in aqueous medium[52]. For Gram-negatives, however, the situation changes in that an external barrier, i.e., the outer membrane (OM), must be disrupted prior to the "lethal hit" i.e., permeabilization of the inner membrane (IM). In this scenario, while high hydrophobicity improves the affinity of the antibiotic peptide for LPS (the major component of the OM), excess affinity may sequester the peptide into the OM, hence precluding its crucial interaction with the IM target. Therefore, a rather subtle balance between hydrophobicity and cationic character is desirable for activity against Gram-negatives[18]. These considerations broadly agree with the finding that peptides **1-5**, more toxic than GS towards erythrocytes (Table 3), are also more hydrophobic than GS by an accepted criterion[23], namely RP-HPLC retention times consistently longer than those of the parent peptide (see Supporting Information, Figure SF1). On the other hand, the D-Tic (**6**) analogue combines decreased cytotoxicity with higher hydrophobicity (longer HPLC retention time) than GS (Table 3). Likewise, the similar HPLC retention times for peptides **1-4** (10.3-10.6 min, Figure SF1) do not correlate well with their antimicrobial profiles. Thus, while **1** improved on GS against all bacteria tested, Nal-containing analogues **2** and **3**, with presumably comparable hydrophobicity, were similar to GS against Gram-positives but practically inactive against Gram-negatives. In conclusion, it appears that, at least for this series, hydrophobicity has limited value in explicating antibiotic performance.

NMR results shed additional light on the structure-activity analysis of the peptides. In particular, they reveal a varying degree of conformational freedom in their side chains that can be reasonably related to differences in antimicrobial activity. For instance, the aromatic ring of the D-Hpa-containing analogue (**1**), separated from the backbone by an extra methylene group, can plausibly explore a larger conformational space and consequently a wider repertoire of membrane (either prokaryotic or eukaryotic) interaction modes than the D-Phe-containing GS, thus explaining its increased activity towards both bacterial and mammalian cells. In contrast, the naphthalene rings in **2** and **3** have conformational freedoms similar in principle to the phenyl group of GS, but their bulkiness is likely to pose a limitation on their interaction with LPS and ensuing OM disruption in Gram-negative bacteria. For Gram-positives, on the other hand, no comparable tightly packed external barrier exists, which would agree with both the preservation of antibiotic activity in both analogues, as well as their hemolytic properties. Similar considerations on the orientation and/or rotational freedom of the aromatic rings can be applied to the contrasting activities of **4** (D-Dip) and **5** (D-Flg). In the latter analogue, the two aromatic rings are fastened into a bulky planar tricylic system, whose predictable sluggishness may help to explain its significantly worse profile than **4**.

By far the most striking result in the present series is the improved therapeutic profile of the D-Tic analogue **6**. With an apparent hydrophobicity (based on RP-HPLC retention time) slightly higher than GS, it is basically equipotent to GS against Gram-positives but has considerably lower toxicity, hence a much better TI (Table 3). From the structural point of view, **6** has two distinctive features over the other analogues in the series. First, the severe conformational restriction on the (proline-like) imino acid D-Tic imposed by the cyclization between the phenyl group and the backbone, and borne out by the observation of practically a single conformer by NMR. Interestingly, the hydrogen-bonding interaction between the δ-amino group of Orn and the backbone carbonyl of D-Phe reported for GS and some analogues[53,54] would thus not be present in analogue **6**. The absence of this favorable effect would most likely be compensated by the stabilizing contribution that the increased rigidity of D-Tic -compared with D-Phe- imparts to the β-turn structure. As a rigid side chain is conceivably more difficult to insert into lipid bilayers than a flexible one (i.e., that of GS), this could account for the lack of hemolytic effect of **6** and thus its improved antibiotic profile. Second, in **6** the δ-NH$_3^+$ groups of Orn are positioned close to the aromatic ring of D-Tic, possibly favored by a π-cation interaction. According to NMR and MD studies on the membrane-bound structure of GS [43,55,56], the peptide lies flat relative to the bilayer plane, near the interface between polar and apolar regions, so that the δ-NH$_3^+$ groups of Orn can interact with phospholipid polar head groups. Now, if a similar contact model is assumed for analogue **6**, the aforementioned π-cation interaction between D-Tic and Orn must disappear. The thermodynamic penalty thus incurred would be higher for the interaction with (zwitterionic) eukaryotic than for prokaryotic membranes, where the loss of the D-Tic – Orn interaction would be compensated by electrostatic attraction between Orn δ-NH$_3^+$ and phosphate head groups. Again, this may account for the higher relative loss in hemolytic than in bactericidal effect.

Conclusions

Analogues of the antimicrobial peptide GS with different aromatic replacements at both D-Phe residues have been synthesized in order to explore how the conformational freedom and the size of the aromatic moiety modulate both biological and structural properties. NMR studies confirmed that the overall molecular shape of the GS framework is maintained in all analogues (some distortion cannot be discarded for the D-Flg derivative), so that variations in antibiotic profile can be ascribed to the different D-Phe replacements. The results suggest that both bulkiness and orientation of the aromatic system at the 4/4′ position are essential for biological activity, to the point that slight modifications in these parameters bring about significant changes in antibacterial activity as well as in the desirable specificity for bacterial over

mammalian cells. An interesting finding is that analogue **6**, with ᴅ-Tic replacing ᴅ-Phe, retains antibiotic potency against Gram-positive bacteria but is hardly cytotoxic. Our NOE data clearly indicate that in this analogue the Orn side chain orientates towards the ᴅ-Tic aromatic rings. A plausible explanation for this orientation is the existence of a cation-π interaction between the δ-NH₃⁺ groups of the Orn side chain and the aromatic ring of ᴅ-Tic. In any event, and regardless of the nature of the interaction, the specific orientation of the ᴅ-Tic aromatic ring relative to the Orn side chain allows explaining the distinct biological behavior exhibited by this peptide. While the increase in therapeutic index relative to GS is only five-fold, it is nonetheless remarkable because, in contrast to other studies[25,42], it has been achieved with minimal alteration of the GS structure, including chirality and cycle size. Modifications of this type may be helpful in understanding the mechanism of action of GS and developing peptide antibiotics with improved pharmaceutical applications.

Experimental Section

Chemicals and instrumentation for peptide synthesis

Fluorenylglycine was prepared as previously reported.[34] *N*-Boc ornithine was purchased from Bachem (Bubendorf, Switzerland) and its side-chain amino group was protected as a formamide by reaction with formic acid and 1,1′-oxalyldiimidazole.[35] All other amino acids were purchased from Senn Chemicals (Dielsdorf, Switzerland), NeoMPS (Strasbourg, France) or Fluka (Buchs, Switzerland). Chloromethylated Merrifield resin and TFMSA were from Fluka, HATU from GenScript (Piscataway, NJ), and HBTU from Matrix Innovation (Montreal, Quebec). Solvents and other chemicals were from SDS (Peypin, France). Mass determination by the MALDI-TOF technique was done in a Voyager DE-RP spectrometer (Applied Biosystems, Foster City, CA) using 2,5-dihydroxybenzoic acid as a matrix. Analytical RP-HPLC was performed on an LC-2010A workstation (Shimadzu Corporation, Kyoto, Japan) with a Luna C₈ (3 μm, 50 × 4.6 mm) column (Phenomenex B.V., Utrecht, The Netherlands) eluted with a linear 5–95% gradient of CH₃CN (+0.036% TFA, v/v) into H₂O (+0.045% TFA, v/v) over 15 min at 1 mL/min flow rate, with UV detection at 220 nm. Preparative RP-HPLC purification was done on a Phenomenex Luna C₈ column (10 μm, 250 × 10 mm) running linear gradients of CH₃CN (+0.1% TFA, v/v) into H₂O (+0.1% TFA, v/v) as indicated for each peptide, at a flow rate of 5 mL/min. The preparative system included two Shimadzu LC-8A pumps, a Shimadzu SPD-10A detector and a Foxy Jr. fraction collector (Teledyne Isco, Lincoln, NE).

General procedure for peptide synthesis

All peptides were synthesized manually by solid-phase methods on a Boc-Pro-Merrifield resin (0.1 mmol) using Boc chemistry. Boc-amino acids (0.3 mmol) were coupled by HBTU/DIEA (0.3 and 0.6 mmol, respectively) for 30–45 min in DMF. HATU was used instead of HBTU for coupling of the 4/4′ residues. To avoid diketopiperazine formation, the third amino acid of each sequence was incorporated by the *in situ* neutralization method[57]. Coupling and deprotection reactions were monitored by the nynhidrin[58] or *p*-nitrophenylester[59] colorimetric tests. The linear decapeptide was cleaved from the resin by treatment with TFA/TFMSA/TIS 10:1:1 (v/v/v) (4 mL) at room temperature for 90 min, then precipitated with cold *tert*-butyl methyl ether. The peptide was redissolved in glacial acetic acid, filtered off the resin and lyophilized. The residue was dissolved in DMF to a final concentration of 2 mg/mL and stirred for 1 h at room temperature in the presence of HBTU/HOBt/DIEA (3:3:5 eq). After solvent removal and lyophilization, the cyclized peptide was deformylated by treatment with 20% hydrochloric acid in methanol at 37°C for 21 h. The solvent was evaporated under reduced pressure, the residue was taken up in glacial acetic acid and lyophilized. Final purification was by preparative reversed-phase HPLC as indicated in each case. HPLC-homogeneous fractions

were combined and lyophilized to give white powders of ≥99% HPLC purity (see Supporting Information, Figure SF2).

cyclo(**Val-Orn-Leu-ᴅ-Phe-Pro)₂** (GS): RP-HPLC, linear 35–70% CH_3CN gradient into H_2O for 30 min (33 mg, 0.029 mmol, 25% overall yield). $[M+H]^+_{calcd} = 1141.7$; $[M+H]^+_{obs} = 1141.1$.

cyclo(**Val-Orn-Leu-ᴅ-Hpa-Pro)₂** (**1**): RP-HPLC, linear 45–75% CH_3CN gradient into H_2O for 30 min (51 mg, 0.044 mmol, 41% overall yield). $[M+H]^+_{calcd} = 1169.7$; $[M+H]^+_{obs} = 1169.5$.

cyclo(**Val-Orn-Leu-ᴅ-1-Nal-Pro)₂** (**2**): RP-HPLC, linear 45–75% CH_3CN gradient into H_2O for 30 min (34 mg, 0.027 mmol, 26% overall yield). $[M+H]^+_{calcd} = 1241.7$; $[M+H]^+_{obs} = 1241.8$.

cyclo(**Val-Orn-Leu-ᴅ-2-Nal-Pro)₂** (**3**): RP-HPLC, linear 45–75% CH_3CN gradient into H_2O for 30 min (26 mg, 0.021 mmol, 20% overall yield). $[M+H]^+_{calcd} = 1241.7$; $[M+H]^+_{obs} = 1241.6$.

cyclo(**Val-Orn-Leu-ᴅ-Dip-Pro)₂** (**4**): RP-HPLC, linear 50–80% CH_3CN gradient into H_2O for 30 min (22 mg, 0.017 mmol, 15% overall yield). $[M+H]^+_{calcd} = 1293.8$; $[M+H]^+_{obs} = 1293.6$.

cyclo(**Val-Orn-Leu-ᴅ-Flg-Pro)₂** (**5**): RP-HPLC, linear 55–85% CH_3CN gradient into H_2O for 30 min (18 mg, 0.015 mmol, 14% overall yield). $[M+H]^+_{calcd} = 1289.7$; $[M+H]^+_{obs} = 1289.8$).

cyclo(**Val-Orn-Leu-ᴅ-Tic-Pro)₂** (**6**): RP-HPLC, linear 45–65% CH_3CN gradient into H_2O for 30 min (23 mg, 0.020 mmol, 19% overall yield). $[M+H]^+_{calcd} = 1165.7$; $[M+H]^+_{obs} = 1165.8$.

NMR spectroscopy

Samples for NMR experiments were prepared at 1–2 mM peptide concentration in 0.5 mL of H_2O/D_2O 9:1 (v/v) or pure D_2O at pH 3.0. pH was measured with a glass microelectrode and was not corrected for isotope effects. NMR spectra were acquired on a Bruker AV 600 MHz spectrometer equipped with a z-gradient cryoprobe. A methanol sample was used to calibrate the temperature of the NMR probe. One-dimensional (1D) and two-dimensional (2D) spectra were acquired by standard pulse sequences using presaturation of the water signal. Mixing times for 2D TOCSY and NOESY were 60 and 150ms, respectively. The ^1H–^{13}C and ^1H–^{15}N HSQC spectra[60] at natural ^{13}C and ^{15}N abundance were recorded in D_2O and H_2O/D_2O 9:1 (v/v), respectively. Data were processed using TOPSPIN (Bruker Biospin, Rheinstetten, Germany) software. Sodium 2,2-dimethyl-2-silapentane-5-sulphonate (DSS) was used as an internal reference for ^1H chemical shifts. The ^{13}C and ^{15}N chemical shifts were indirectly calibrated by multiplying the spectrometer frequency that corresponds to 0 ppm in the ^1H spectrum, assigned to internal DSS reference, by 0.25144954 and 0.101329118, respectively.[61]

The ^1H-NMR signals of the peptides were assigned by sequential assignment methods.[62] The ^{13}C and ^{15}N resonances were then assigned following the cross-correlations observed in the HSQC spectra between the proton and the hetero-nucleus to which it is bonded.

To measure the NH/ND exchange rates, a freeze-dried sample of peptide GS was solved in pure D_2O at pH 3.0, and after the 10–15 min required to set up the NMR experiment consecutive 1D and 2D 20ms-TOCSY spectra were recorded at 5 °C.

Structure calculation

Structure calculations were performed by using the CYANA program[63] and an annealing strategy. Since the non-proteinogenic amino acids were not included in the standard CYANA libraries, we built them using MOLMOL[64] and manual optimization (these libraries are available upon request from the authors). For this purpose, X-ray data of compounds containing these amino acids were retrieved from the Cambridge Structural Database[65]. Theoretical constraints for the GS β-sheet incorporated for structure calculation included (φ) and ψ angle restraints, lower and upper-limit distance restraints for the four characteristic cross-strand hydrogen-bonds, and upper-limit distance restraints for the backbone atoms of strand residues (Table ST4). Experimental distance constraints were derived from 2D NOESY spectra recorded in H_2O, also in D_2O for analogue **6**. The NOE cross-peaks were integrated by using the automatic integration subroutine of the Sparky program (T.D. Goddard & S.G. Kneller, University of California at San Francisco) and then calibrated and converted to upper-limit distance constraints with CYANA[63]. Given the symmetrical nature of the peptides, for structure calculations residues were re-numbered from 1 to 10 starting at Leu3 (Figure 1). Lower and upper limit restraints required for peptide backbone cyclization were introduced with CYANA[63] (see Supporting Information). For each peptide, a total of 50 conformers were generated and the 20 conformers with the lowest target function were analyzed. Model structures for GS and analogues **1–6** were examined with MOLMOL. A side chain torsion angle was considered as well defined when its root mean square deviation between values in the 20 best calculated structures was less than ±30°.

Antimicrobial activity

Stocks of *Staphylococcus aureus* CECT 240, *Listeria monocytogenes* CECT 4032, *Acinetobacter baumannii* ATCC 19606 and its isogenic colistin-resistant strain 19606R (obtained by continuous growing under increasing colistin concentration) were maintained at -80 °C in freezing medium (65% glycerol, 0.1 M $MgSO_4$, 25 mM Tris-HCl, pH 8.0). Two days prior to the assay for microbicidal activity, they were thawed and grown in MBH medium (Mueller-Hinton II Broth Cation Adjusted (Becton-Dickinson, Cockeysville, MD) at 37 °C; for 19606R, 64 μg/mL colistin sulfate (Sigma, Madrid, Spain) was included[41]. Bacterial cells were harvested at exponential growth phase, washed twice with phosphate buffered saline (PBS, 10 mM Na_2HPO_4, 1 mM KH_2PO_4, 140 mM NaCl, 3 mM KCl, pH 7.0) and resuspended in MBH, at 5×10^5 CFU/mL. Aliquots (100 μL) from this suspension were transferred into a polypropylene 96 well plate, and bacteria were allowed to proliferate for 24 h at 37 °C in the presence of the corresponding analogue concentration. Afterwards, growth was measured by turbidimetry at 600 nm in a model 680 microplate reader (Bio-Rad Laboratories, Hercules. CA). MIC_{50} was defined as the lowest peptide concentration inhibiting bacterial growth by 50%, relative to untreated control, and was calculated using the SigmaPlot (Systat Software, San Jose, CA) software, v. 9.0.

Hemolytic activity assay

Hemolytic activity of the peptides was determined by triplicate. Defibrinated sheep blood (Biomedics, Madrid, Spain) was centrifuged and washed twice with Hank's medium (136 mM NaCl; 4.2 mM Na_2HPO_4; 4.4 mM KH_2PO_4; 5.4 mM KCl; 4.1 mM $NaHCO_3$, pH 7.2), supplemented with 20 mM D-glucose (Hank's-Glc). Erythrocytes were resuspended in the same buffer at 2×10^7 erythrocytes/mL and 100 μL-aliquots of the suspension were incubated with the peptides (4 h, 37 °C). The remaining erythrocytes were harvested in a Micro 200 microfuge (A. Hettich GmbH & Co KG, Germany) (14,000 rpm, 5 min, 4 °C), 80 μL of the supernatant were transferred into a 96-well culture microplate, and hemoglobin release was read at 550 nm in a Bio Rad 680 (Hercules, CA) microplate reader. The asymptotic ordinate of the GS

supernatant was taken as 100% hemolysis. HC_{50} values were calculated using SigmaPlot, version 9.0.

Supplementary Material

Refer to Web version on PubMed Central for supplementary material.

Acknowledgements

References

1. Hirsch T, Jacobsen F, Steinau HU, Steinstraesser L. Host defense peptides and the new line of defence against multiresistant infections. Protein Pept Lett 2008;15:238–243. [PubMed: 18336350]

2. Parisien A, Allain B, Zhang J, Mandeville R, Lan CQ. Novel alternatives to antibiotics: bacteriophages, bacterial cell wall hydrolases, and antimicrobial peptides. J Appl Microbiol 2008;104:1–13. [PubMed: 18171378]

3. Gause GF. Gramicidin S and its use in the treatment of infected wounds. Nature 1944;154:703.

4. Kondejewski LH, Farmer SW, Wishart DS, Hancock RE, Hodges RS. Gramicidin S is active against both gram-positive and gram-negative bacteria. Int J Pept Protein Res 1996;47:460–466. [PubMed: 8836773]

5. Prenner EJ, Lewis RN, McElhaney RN. The interaction of the antimicrobial peptide gramicidin S with lipid bilayer model and biological membranes. Biochim Biophys Acta 1999;1462:201–221. [PubMed: 10590309]

6. Hull SE, Karlsson R, Main P, Woolfson MM, Dodson EJ. The crystal structure of a hydrated gramicidin S-urea complex. Nature 1978;275:206–207.

7. Schmidt GM, Hodgkin DC, Oughton BM. A crystallographic study of some derivatives of gramicidin S. Biochem J 1957;65:744–750. [PubMed: 13426094]

8. Tishchenko GN, Andrianov VI, Vainstein BK, Woolfson MM, Dodson E. Channels in the gramicidin S-with-urea structure and their possible relation to transmembrane ion transport. Acta Crystallogr D Biol Crystallogr 1997;53:151–159. [PubMed: 15299949]

9. Ovchinnikov YA, Ivanov VT. Conformational states and biological activity of cyclic peptides. Tetrahedron 1975;31:2177–2209.

10. Katsu T, Kobayashi H, Fujita Y. Mode of action of gramicidin S on *Escherichia coli* membrane. Biochim Biophys Acta 1986;860:608–619. [PubMed: 2427118]

11. Afonin S, Glaser RW, Berditchevskaia M, Wadhwani P, Guhrs KH, Mollmann U, Perner A, Ulrich AS. 4-fluorophenylglycine as a label for ^{19}F NMR structure analysis of membrane-associated peptides. Chembiochem 2003;4:1151–1163. [PubMed: 14613106]

12. Arai T, Imachi T, Kato T, Ogawa HI, Fujimoto T, Nishino N. Synthesis of [hexafluorovalyl[1,1']] gramicidin S. Bull Chem Soc Jpn 1996;69:1383–1389.

13. Waki M, Abe O, Okawa R, Kato T, Makisumi S, Izumiya N. Studies of peptide antibiotics. XII. Syntheses of [2,2'-α,γ-diaminobutyric acid]-and[2,2'-lysine]-gramicidin S. Bull Chem Soc Jpn 1967;40:2904–2909. [PubMed: 5588231]

14. Aimoto S. The synthesis of a heavy-atom derivative of gramicidin S (GS), [d-Phe(4-Br)[4,4']]-GS, by a novel method. Bull Chem Soc Jpn 1988;61:2220–2222.

15. Andreu D, Ruiz S, Carreño C, Alsina J, Albericio F, Jiménez MA, de la Figuera N, Herranz R, García-López MT, González-Muñiz R. IBTM-containing gramicidin S analogues: Evidence for IBTM as a suitable type II′ β-turn mimetic. J Am Chem Soc 1997;119:10579–10586.

16. Grotenbreg GM, Buizert AE, Llamas-Saiz AL, Spalburg E, van Hooft PA, de Neeling AJ, Noort D, van Raaij MJ, van der Marel GA, Overkleeft HS, Overhand M. β-Turn modified gramicidin S analogues containing arylated sugar amino acids display antimicrobial and hemolytic activity comparable to the natural product. J Am Chem Soc 2006;128:7559–7565. [PubMed: 16756311]

17. Kawai M, Yamamura H, Tanaka R, Umemoto H, Ohmizo C, Higuchi S, Katsu T. Proline residue-modified polycationic analogs of gramicidin S with high antibacterial activity against both Gram-positive and Gram-negative bacteria and low hemolytic activity. J Pept Res 2005;65:98–104. [PubMed: 15686540]

18. Lee DL, Hodges RS. Structure-activity relationships of de novo designed cyclic antimicrobial peptides based on gramicidin S. Biopolymers 2003;71:28–48. [PubMed: 12712499]

19. Ripka WC, Delucca GV, Bach AC, Pottorf RS, Blaney JM. Protein β-turn mimetics II: Design, synthesis and evaluation in the cyclic peptide gramicidin S. Tetrahedron 1993;49:3609–3628.

20. Sato K, Kato R, Nagai U. Studies on β-turn of peptides. XII. Synthetic conformation of weak activity of [D-Pro$^{5,5'}$]-Gramicidin S predicted from β-turn preference of its partial sequence. Bull Chem Soc Jpn 1986;59:535–538.

21. Tamaki M, Okitsu T, Araki M, Sakamoto H, Takimoto M, Muramatsu I. Synthesis and properties of gramicidin S analogs containing Pro-d-Phe sequence in place of d-Phe-Pro sequence in the β-turn part of the antibiotic. Bull Chem Soc Jpn 1985;58:531–535.

22. Wishart DS, Kondejewski LH, Semchuk PD, Sykes BD, Hodges RS. A method for the facile solid-phase synthesis of gramicidin S and its analogs. Lett Pept Sci 1996;3:53–60.

23. Yamada K, Shinoda SS, Oku H, Komagoe K, Katsu T, Katakai R. Synthesis of low-hemolytic antimicrobial dehydropeptides based on gramicidin S. J Med Chem 2006;49:7592–7595. [PubMed: 17181140]

24. Jelokhani-Niaraki M, Kondejewski LH, Farmer SW, Hancock RE, Kay CM, Hodges RS. Diastereoisomeric analogues of gramicidin S: structure, biological activity and interaction with lipid bilayers. Biochem J 2000;349:747–755. [PubMed: 10903135]

25. Kondejewski LH, Jelokhani-Niaraki M, Farmer SW, Lix B, Kay CM, Sykes BD, Hancock RE, Hodges RS. Dissociation of antimicrobial and hemolytic activities in cyclic peptide diastereomers by systematic alterations in amphipathicity. J Biol Chem 1999;274:13181–13192. [PubMed: 10224074]

26. Abraham T, Marwaha S, Kobewka DM, Lewis RN, Prenner EJ, Hodges RS, McElhaney RN. The relationship between the binding to and permeabilization of phospholipid bilayer membranes by GS14dK4, a designed analog of the antimicrobial peptide gramicidin S. Biochim Biophys Acta 2007;1768:2089–2098. [PubMed: 17686454]

27. Abe O, Izumiya N. Studies of peptide antibiotics. Analogs of gramicidin S containing glycine or alanine in place of leucine. Bull Chem Soc Jpn 1970;43:1202–1207.

28. Prenner EJ, Lewis RN, Kondejewski LH, Hodges RS, McElhaney RN. Differential scanning calorimetric study of the effect of the antimicrobial peptide gramicidin S on the thermotropic phase behavior of phosphatidylcholine, phosphatidylethanolamine and phosphatidylglycerol lipid bilayer membranes. Biochim Biophys Acta 1999;1417:211–223. [PubMed: 10082797]

29. Graciani NR, Tsang KY, McCutchen SL, Kelly JW. Amino acids that specify structure through hydrophobic clustering and histidine-aromatic interactions lead to biologically active peptidomimetics. Bioorg Med Chem 1994;2:999–1006. [PubMed: 7712134]

30. Kee KS, Jois SD. Design of β-turn based therapeutic agents. Curr Pharm Des 2003;9:1209–1224. [PubMed: 12769748]

31. Xiao J, Weisblum B, Wipf P. Trisubstituted (E)-alkene dipeptide isosteres as beta-turn promoters in the gramicidin S cyclodecapeptide scaffold. Org Lett 2006;8:4731–4734. [PubMed: 17020289]

32. Grotenbreg GM, Spalburg E, de Neeling AJ, van der Marel GA, Overkleeft HS, van Boom JH, Overhand M. Synthesis and biological evaluation of novel turn-modified gramicidin S analogues. Bioorg Med Chem 2003;11:2835–2841. [PubMed: 12788356]

33. Shimohigashi Y, Kodama H, Imazu S, Horimoto H, Sakaguchi K, Waki M, Uchida H, Kondo M, Kato T, Izumiya N. [4,4′-(Z)-dehydrophenylalanine]gramicidin S with stabilized bioactive conformation and strong antimicrobial activity. FEBS Lett 1987;222:251–255. [PubMed: 2443391]

34. Royo S, Jiménez AI, Cativiela C. Synthesis of enantiomerically pure β,β-diphenylalanine (Dip) and fluorenylglycine (Flg). Tetrahedron-Asymmetry 2006;17:2393–2400.

35. Kitagawa T, Arita J, Nogahata A. Convenient one-pot method for formylation of amines and alcohols using formic acid and 1,1′-oxalyldiimidazole. Chem Pharm Bull (Tokyo) 1994;42:1655–1657.

36. Schubert M, Labudde D, Oschkinat H, Schmieder P. A software tool for the prediction of Xaa-Pro peptide bond conformations in proteins based on ^{13}C chemical shift statistics. J Biomol NMR 2002;24:149–154. [PubMed: 12495031]

37. Santiveri CM, Rico M, Jiménez MA. ^{13}C$_\alpha$ and ^{13}C$_\beta$ chemical shifts as a tool to delineate β-hairpin structures in peptides. J Biomol NMR 2001;19:331–345. [PubMed: 11370779]

38. Wishart DS, Sykes BD, Richards FM. Relationship between nuclear magnetic resonance chemical shift and protein secondary structure. J Mol Biol 1991;222:311–333. [PubMed: 1960729]

39. Santiveri CM, Rico M, Jiménez MA. Position effect of cross-strand side-chain interactions on beta-hairpin formation. Protein Sci 2000;9:2151–2160. [PubMed: 11152125]

40. Wishart DS, Bigam CG, Holm A, Hodges RS, Sykes BD. ^{1}H, ^{13}C and ^{15}N random coil NMR chemical shifts of the common amino acids. I. Investigations of nearest-neighbor effects. J Biomol NMR 1995;5:67–81. [PubMed: 7881273]

41. Saugar JM, Rodríguez-Hernández MJ, de la Torre BG, Pachón-Ibáñez ME, Fernández-Reyes M, Andreu D, Pachón J, Rivas L. Activity of cecropin A-melittin hybrid peptides against colistin-resistant clinical strains of *Acinetobacter baumannii*: molecular basis for the differential mechanisms of action. Antimicrob Agents Chemother 2006;50:1251–1256. [PubMed: 16569836]

42. Kondejewski LH, Lee DL, Jelokhani-Niaraki M, Farmer SW, Hancock REW, Hodges RS. Optimization of microbial specificity in cyclic peptides by modulation of hydrophobicity within a defined structural framework. J Biomol Chem 2002;1:67–74.

43. McInnes C, Kondejewski LH, Hodges RS, Sykes BD. Development of the structural basis for antimicrobial and hemolytic activities of peptides based on gramicidin S and design of novel analogs using NMR spectroscopy. J Biol Chem 2000;275:14287–14294. [PubMed: 10799508]

44. Bach AC, Markwalder JA, Ripka WC. Synthesis and NMR conformational analysis of a β-turn mimic incorporated into gramicidin S - A general approach to evaluate β-turn peptidomimetics. Int J Pept Protein Res 1991;38:314–323. [PubMed: 1724663]

45. Estiarte MA, Rubiralta M, Díez A, Thormann M, Giralt E. Oxazolopiperidin-2-ones as type II′ β-turn mimetics: Synthesis and conformational analysis. J Org Chem 2000;65:6992–6999. [PubMed: 11031021]

46. Gibbs AC, Bjorndahl TC, Hodges RS, Wishart DS. Probing the structural determinants of type II′ β-turn formation in peptides and proteins. J Am Chem Soc 2002;124:1203–1213. [PubMed: 11841288]

47. Matsuura S, Waki M, Izumiya N. Studies of peptide antibiotics. XXVII. Synthesis of an analog of gramicidin S containing a glycine residue in place of a proline. Bull Chem Soc Jpn 1972;45:863–866.

48. Higashijima T, Miyazawa T, Kawai M, Nagai U. Gramicidin S analogs with a d-Ala, Gly, or l-Ala residue in place of the d-Phe residue: molecular conformations and interactions with phospholipid membrane. Biopolymers 1986;25:2295–2307. [PubMed: 2432956]

49. Aarstad K, Zimmer TL, Laland SG. Replacement of phenylalanine in gramicidin S by other amino acids. FEBS Lett 1979;103:118–121. [PubMed: 89046]

50. Ando S, Aoyagi H, Waki M, Kato T, Izumiya N. Studies of peptide antibiotics. XLIII. Syntheses of gramicidin S analogs containing D-serine or dehydroalanine in place of d-phenylalanine and asymmetric hydrogenation of the dehydroalanine residue. Int J Pept Protein Res 1983;21:313–321. [PubMed: 6189795]

51. Wu M, Maier E, Benz R, Hancock RE. Mechanism of interaction of different classes of cationic antimicrobial peptides with planar bilayers and with the cytoplasmic membrane of *Escherichia coli*. Biochemistry 1999;38:7235–7242. [PubMed: 10353835]

52. Lee DL, Powers JP, Pflegerl K, Vasil ML, Hancock RE, Hodges RS. Effects of single D-amino acid substitutions on disruption of beta-sheet structure and hydrophobicity in cyclic 14-residue

antimicrobial peptide analogs related to gramicidin S. J Pept Res 2004;63:69–84. [PubMed: 15009528]

53. Krauss EM, Chan SI. Intramolecular hydrogen bonding in gramicidin S. 2. Ornithine. J Am Chem Soc 1982;104:6953–6961.

54. Yamada K, Unno M, Kobayashi K, Oku H, Yamamura H, Araki S, Matsumoto H, Katakai R, Kawai M. Stereochemistry of protected ornithine side chains of gramicidin S derivatives: X-ray crystal structure of the bis-Boc-tetra-N-methyl derivative of gramicidin S. J Am Chem Soc 2002;124:12684–12688. [PubMed: 12392415]

55. Salgado J, Grage SL, Kondejewski LH, Hodges RS, McElhaney RN, Ulrich AS. Membrane-bound structure and alignment of the antimicrobial beta-sheet peptide gramicidin S derived from angular and distance constraints by solid state 19F-NMR. J Biomol NMR 2001;21:191–208. [PubMed: 11775737]

56. Mihailescu D, Smith JC. Atomic detail peptide-membrane interactions: molecular dynamics simulation of gramicidin S in a DMPC bilayer. Biophys J 2000;79:1718–1730. [PubMed: 11023880]

57. Schnölzer M, Alewood P, Jones A, Alewood D, Kent SB. In situ neutralization in Boc-chemistry solid phase peptide synthesis. Rapid, high yield assembly of difficult sequences. Int J Pept Protein Res 1992;40:180–193. [PubMed: 1478777]

58. Kaiser E, Colescott RL, Bossinger CD, Cook PI. Color test for detection of free terminal amino groups in solid-phase synthesis of peptides. Anal Biochem 1970;34:595–598. [PubMed: 5443684]

59. Madder A, Farcy N, Hosten NGC, De Muynck H, De Clercq PJ, Barry J, P DA. A novel sensitive colorimetric assay for visual detection of solid phase bound amines. Eur J Org Chem 1999:2787–2791.

60. Bax A, Lerner L. Two-dimensional nuclear magnetic resonance spectroscopy. Science 1986;232:960–967. [PubMed: 3518060]

61. Markley JL, Bax A, Arata Y, Hilbers CW, Kaptein R, Sykes BD, Wright PE, Wüthrich K. Recommendations for the presentation of NMR structures of proteins and nucleic acids--IUPAC-IUBMB-IUPAB Inter-Union Task Group on the standardization of data bases of protein and nucleic acid structures determined by NMR spectroscopy. J Biomol NMR 1998;12:1–23. [PubMed: 9729785]

62. Wüthrich K, Billeter M, Braun W. Polypeptide secondary structure determination by nuclear magnetic resonance observation of short proton-proton distances. J Mol Biol 1984;180:715–740. [PubMed: 6084719]

63. Güntert P. Automated NMR structure calculation with CYANA. Methods Mol Biol 2004;278:353–378. [PubMed: 15318003]

64. Koradi R, Billeter M, Wüthrich K. MOLMOL: a program for display and analysis of macromolecular structures. J Mol Graph 1996;14:51–55. 29–32. [PubMed: 8744573]

65. Allen FH. The Cambridge Structural Database: a quarter of a million crystal structures and rising. Acta Crystallogr B 2002;58:380–388. [PubMed: 12037359]
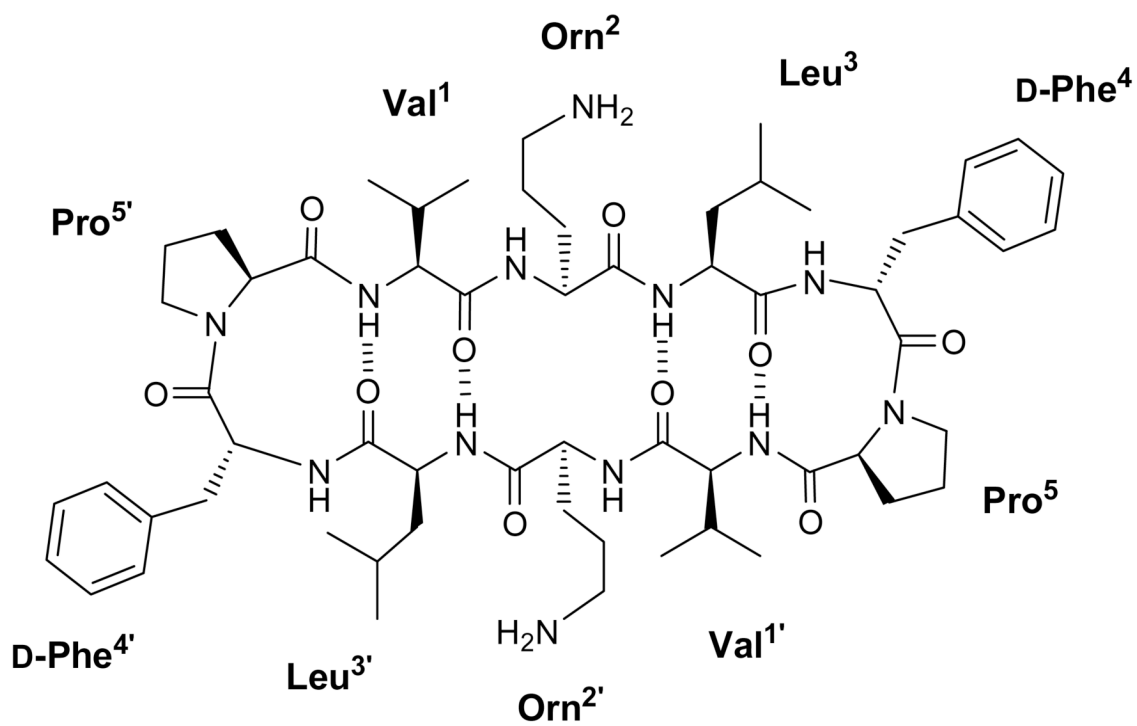
Abbreviations

ATCC

American Type Culture Collection

Boc

tert-butoxycarbonyl

CECT

Spanish Type Culture Collection

COSY

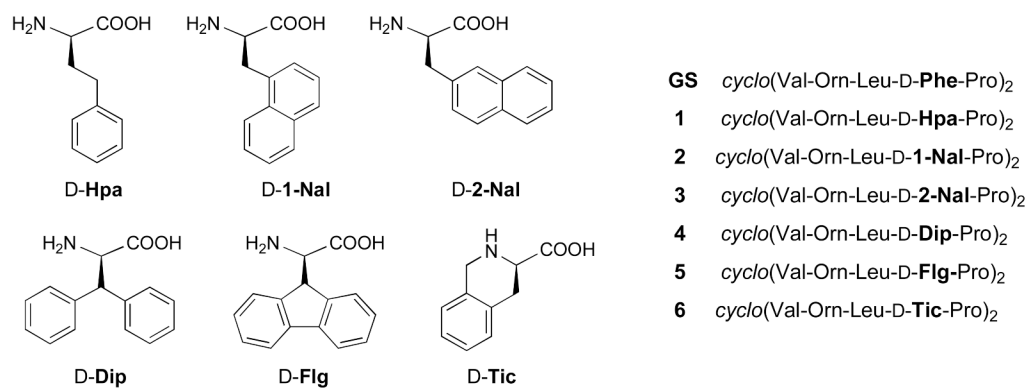correlated spectroscopy

DIEA

N,N-diisopropylethylamine

Dip

β,β-diphenylalanine

DMF

N,N-dimethylformamide

DSS

2,2-dimethyl-2-silapentane-5-sulphonate

Flg

fluorenylglycine

For

formyl

GS

gramicidin S

HATU

2-(7-aza-1*H*-benzotriazole-1-yl)-1,1,3,3-tetramethyluronium hexafluorophosphate

HBTU

2-(1*H*-benzotriazole-1-yl)-1,1,3,3-tetramethyluronium hexafluorophosphate

HC$_{50}$

50% hemolytic concentration

HOBt

N-hydroxybenzotriazole

Hpa

homophenylalanine

HSQC

heteronuclear single quantum coherence spectra

IM

inner membrane

LPS

lipopolysacharide

MALDI-TOF

matrix-assisted laser desorption ionization-time of flight

MIC$_{50}$

minimal inhibitory concentration

1-Nal

1-naphthylalanine

2-Nal

2-naphthylalanine

NOESY

nuclear Overhauser enhancement spectroscopy

OM

outer membrane

Orn

ornithine

Phg

phenylglycine

PXE

polymyxin E

RMSD

root mean square deviation

SAR

structure-activity relationship

TFA

trifluoroacetic acid

TFMSA

trifluoromethanesulfonic acid

TI

therapeutic index $(=HC_{50}/MIC_{50})$

Tic

1,2,3,4-tetrahydroisoquinoline-3-carboxylic acid

TIS
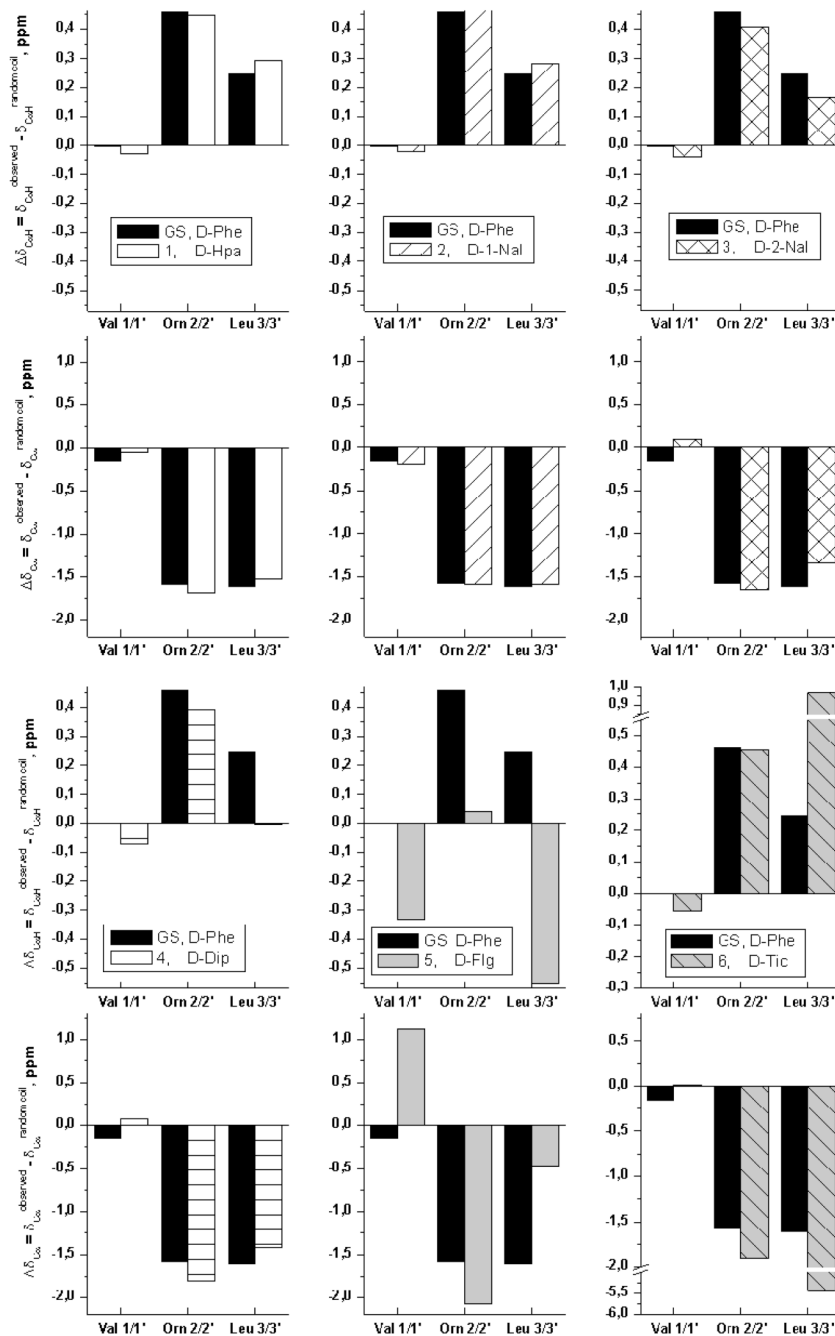
triisopropylsilane

TOCSY

total correlated spectroscopy

Figure 1.
β-sheet structure of gramicidin S.

|	
GS	*cyclo*(Val-Orn-Leu-D-**Phe**-Pro)$_2$
1	*cyclo*(Val-Orn-Leu-D-**Hpa**-Pro)$_2$
2	*cyclo*(Val-Orn-Leu-D-**1-Nal**-Pro)$_2$
3	*cyclo*(Val-Orn-Leu-D-**2-Nal**-Pro)$_2$
4	*cyclo*(Val-Orn-Leu-D-**Dip**-Pro)$_2$
5	*cyclo*(Val-Orn-Leu-D-**Flg**-Pro)$_2$
6	*cyclo*(Val-Orn-Leu-D-**Tic**-Pro)$_2$

Figure 2.
Amino acids selected as D-Phe replacements for GS analogues **1-6**.

Figure 3.
Histograms showing the $\Delta\delta_{C\alpha H}$ and $\Delta\delta_{C\alpha}$ profiles ($\Delta\delta = \delta^{observed} - \delta^{random\ coil}$, ppm) for GS (black bars) and its analogues (patterned or colored bars as indicated in the corresponding insets) in aqueous solution at pH 3.0 and 5°C. Lys $\delta^{random\ coil}$ values[40] were used to calculate the $\Delta\delta$ values for the Orn residues.
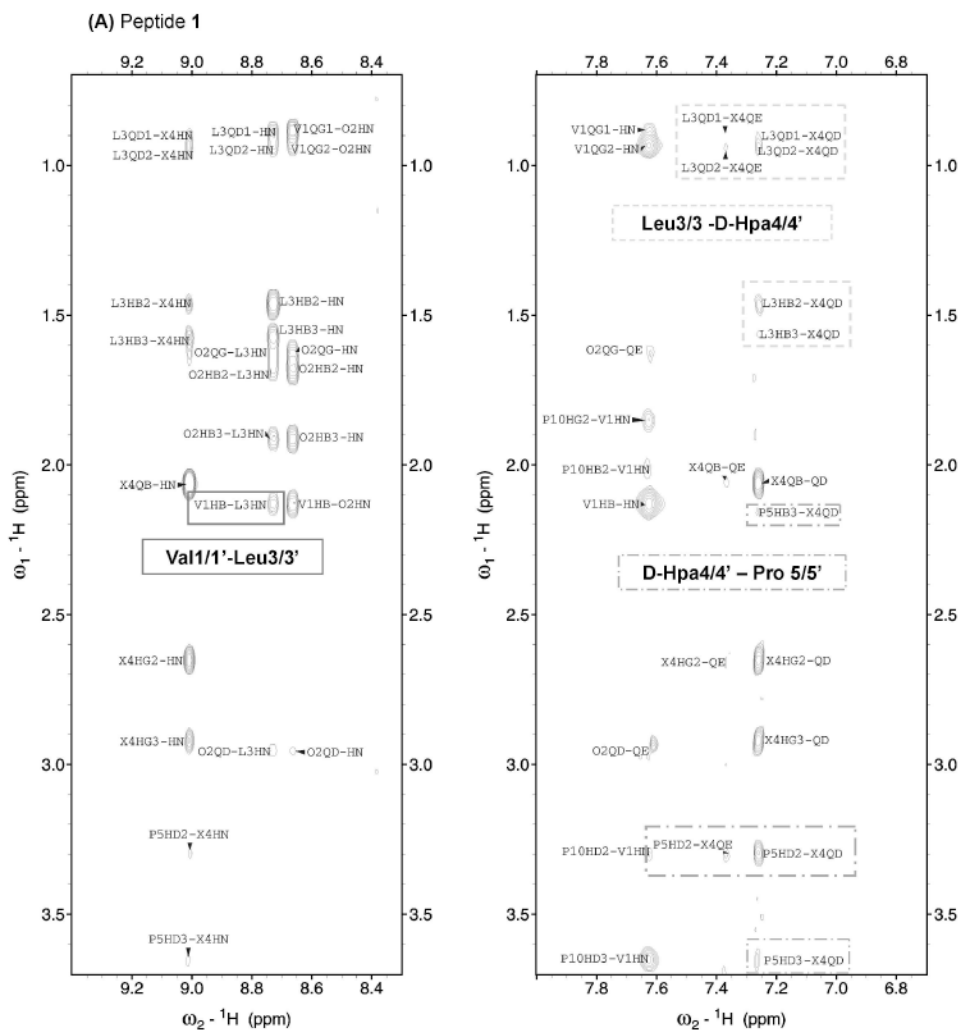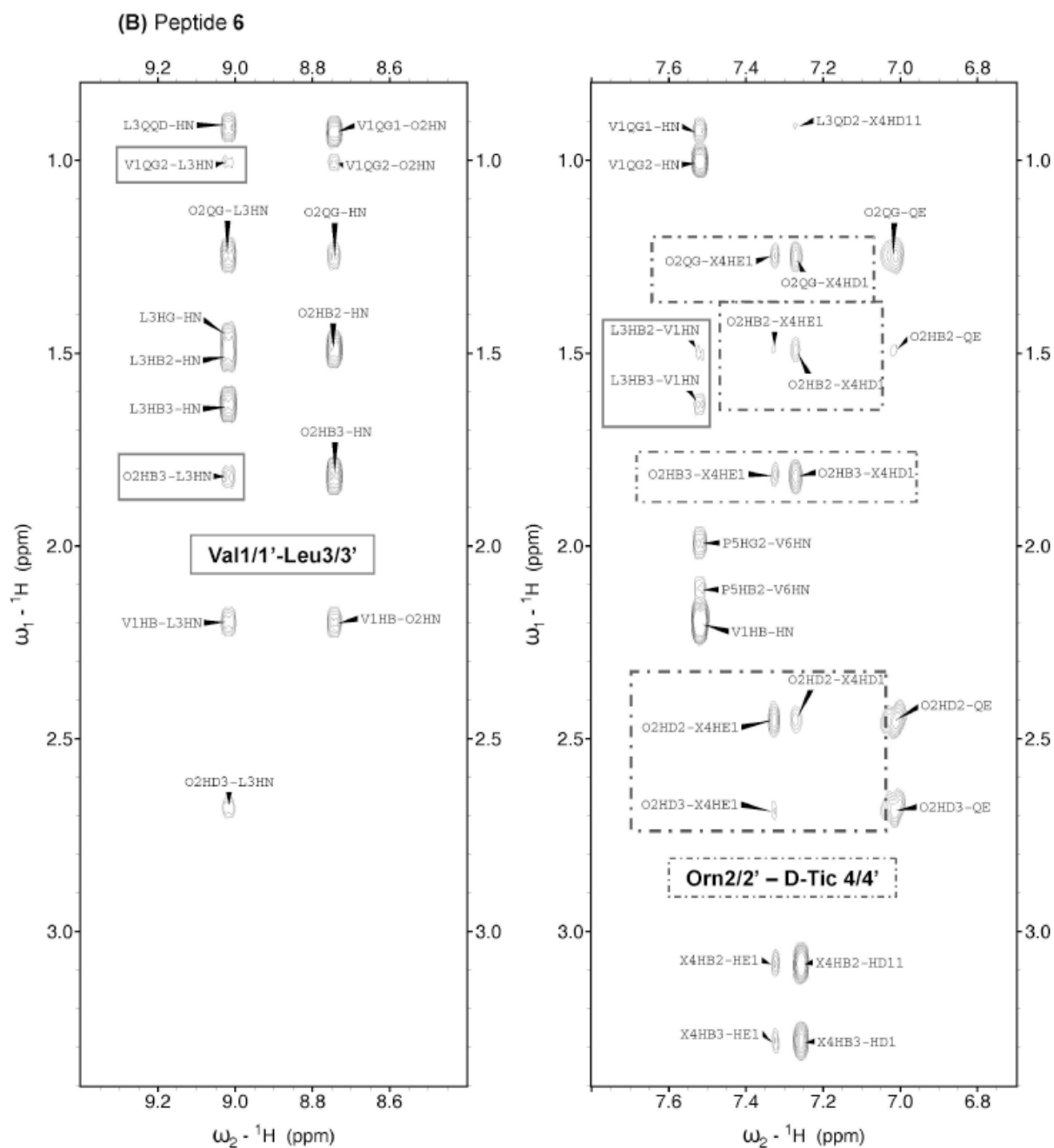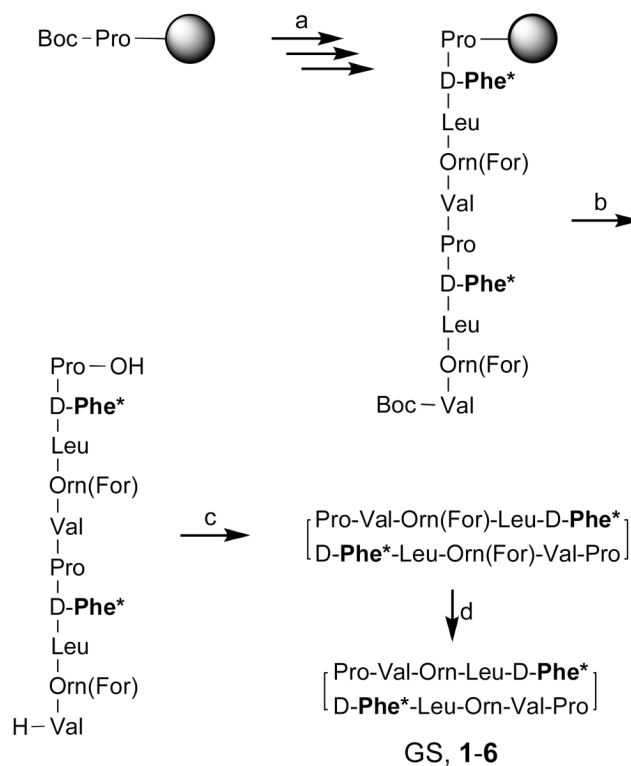
(A) Peptide **1**

Figure 4.
Selected NOESY spectral regions for peptides **1** (A) and **6** (B) in H$_2$O/D$_2$O 9:1 v/v at pH 3 and 5 °C. Relevant sequential and non-sequential NOEs are boxed.
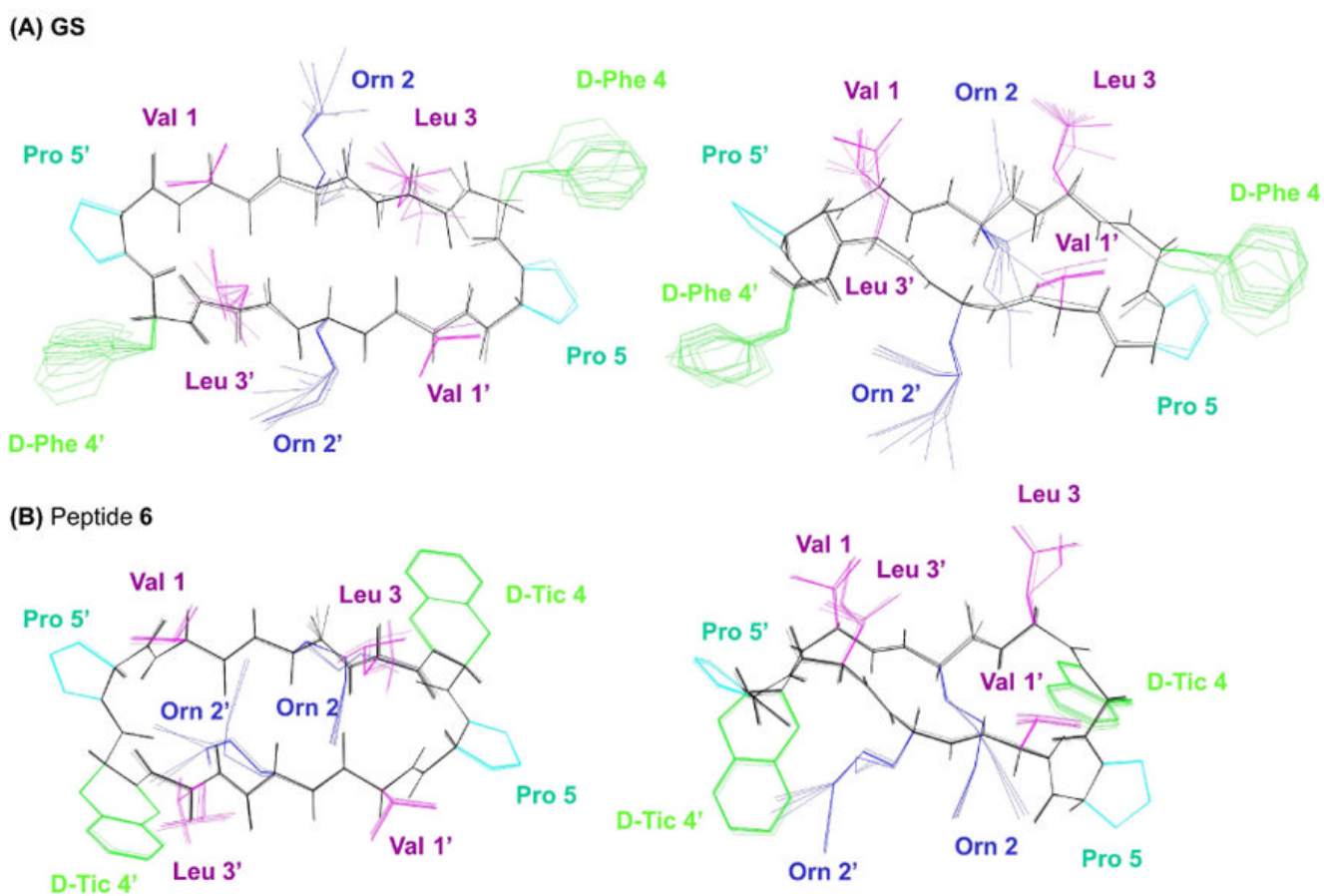
Figure 5.
Model structures for GS (A) and peptide **6** (B) in two different views. Backbone atoms are shown in black. Side chains for aromatic D-Phe and D-Tic are colored in green, for Pro in cyan, for Orn in red, and for Leu and Val in magenta.

Scheme 1.

Synthetic strategy for GS and its analogues[a]

[a]Reagents and conditions: (a) standard solid-phase peptide synthesis (Boc chemistry); (b) TFA/ TFMSA/TIS 10:1:1, rt, 90 min; (c) HBTU/HOBt/DIEA (3:3:5 eq), DMF, rt, 1 h; (d) 20% HCl in MeOH, 37°C, 21 h. D-Phe* stands for D-Phe or the corresponding substitute.

Table 1

Summary of NOEs observed for GS and peptides **1-6**. Observation of one or more NOE involving at least one side chain proton of the indicated residues is shown by a "+". D-Phe* stands for D-Phe or the corresponding substitute. "Ov" indicates signal overlapping. "w" and "vw" indicates weak and very weak peak intensities, respectively.

NOE	GS D-Phe	1 D-Hpa	2[a] D-1-Nal	3 D-2-Nal	4 D-Dip	5 D-Flg	6 D-Tic
NH Val1 – NH Leu3'/NH Val1' – NH Leu3	+	+	----	+(vw)	----	Ov	+
Val1/1' – Leu3/3'	+	+	----	+	+	+	+
Orn2/2' – DPhe*4/4'	----	----	----	----	----	----	+
Leu3/3' – DPhe*4/4'	+	+	+(w)	+	+	+	+(vw)
DPhe*4/4' – Pro5/5'	+	+	----	+	+	+	----

[a] Signal-to-noise ratio is poor in NOESY spectra of peptide **2** as a consequence of its low solubility.

Table 2

Temperature coefficients[a] ($\Delta\delta/\delta T$, ppb.K^{-1}) for amide protons in GS and its analogues.

Peptide	D-Phe*[b]	Val[1,1'](NH)	Orn[2,2'](NH)	Leu[3,3'](NH)	D-Phe*[4,4'](NH)
GS	D-Phe	−7.4	−7.1	−0.8	−8.6
1	D-Hpa	−6.1	−7.8	−1.2	−11.0
2	D-1-Nal	−8.0	−7.0	−1.5	−8.0
3	D-2-Nal	−11.4	−6.6	0.2	−7.6
4	D-Dip	−13.4	−7.3	−1.7	−10.1
5	D-Flg	−23.4	−3.6	0.0	c
6	D-Tic	−1.3	−8.0	−3.9	—

[a]Measured in H$_2$O/D$_2$O 9:1 (v/v) at pH 3.0.

[b]D-Phe* stands for D-Phe or the corresponding substitute.

[c]Not determined; NH protons not observed at 25 °C probably because of fast exchange with water.

Table 3

Cytotoxic (hemolytic) and antimicrobial activity of GS and analogues

Peptide	D-Phe*[a]	Erythrocytes	S. aureus		L. monocytogenes		A. baumanni S		A. baumannii R[e]	
		HC_{50}^{b} (µM)	MIC_{50}^{c} (µM)	TI^{d}	MIC_{50} (µM)	TI	MIC_{50} (µM)	TI	MIC_{50} (µM)	TI
GS	D-Phe	21.1 (± 2.6)	7.9 (± 0.8)	2.7 (1)	6.7 (± 0.2)	3.1 (1)	10.1 (± 0.4)	2.1 (1)	13.1 (± 0.0)	1.6 (1)
1	D-Hpa	7.0 (± 0.3)	3.5 (± 0.1)	2 (0.7)	2.4 (± 0.0)	2.9 (0.9)	4.6 (± 0.1)	1.5 (0.7)	6.2 (± 0.1)	1.1 (0.7)
2	D-1-Nal	5.0 (± 0.1)	2.9 (± 0.5)	1.7 (0.6)	8.6 (± 0.6)	0.6 (0.2)	35.9 (± 0.0)	0.1 (0.0)	>40	>0.1
3	D-2-Nal	7.1 (± 3.5)	4.6 (± 0.6)	1.5 (0.6)	7.8 (± 0.4)	0.9 (0.3)	39.6 (± 0.0)	0.2 (0.1)	>40	>0.2
4	D-Dip	8.6 (± 1.1)	3.4 (± 0.0)	2.5 (0.9)	7.7 (± 0.6)	1.1 (0.4)	9.6 (± 0.9)	0.9 (0.4)	17.8 (± 0.0)	0.5 (0.3)
5	D-Flg	6.2 (± 0.3)	8 (± 0.0)	0.8 (0.3)	9.2 (±1.4)	0.7 (0.2)	15.4 (± 1.3)	0.4 (0.2)	>40	>0.1
6	D-Tic	>50	4.9 (±0.4)	>10.2 (3.8)	8.3 (± 0.5)	>6 (2.0)	>40	>ND	>40	ND

[a] D-Phe* stands for D-Phe or the corresponding substitute.

[b] HC50: peptide concentration required for 50% lysis of sheep erythrocytes.

[c] MIC50: peptide concentration required for 50% inhibition of bacterial growth after 24 h, relative to a control culture.

[d] TI (therapeutic index)= HC50/MIC50

[e] An A. baumannii strain resistant to polymyxin E (colistin). ND, not determined. Standard deviations (SD) are shown in parentheses.